Magnetodynamics

All-Angle Collimation for Spin Waves

Jarosław W. Kłos, Pawel Gruszecki, Andriy E. Serebryannikov, and Maciej Krawczyk

Faculty of Physics, Adam Mickiewicz University in Poznań, 61-614 Poznań, Poland

Received 15 Sep 2015, revised 15 Oct 2015, accepted 20 Oct 2015, published 26 Oct 2015, current version 9 Dec 2015.

Abstract— Collimation of monochromatic beams of spin waves results from refraction at the interface between two magnetic half-planes. Collimation occurs for a broad range of the angles of incidence for homogenous Co and Permalloy (Py) half-planes due to the intrinsic anisotropy of spin-wave propagation in these materials. The effect arises in samples saturated by an in-plane magnetic field tangential to the interface. Further, collimation for all possible angles of incidence occurs in a system where the incident spin wave is refracted at the interface between homogeneous and periodically patterned layers of yttrium–iron garnet (YIG). The refraction was investigated by the analysis of isofrequency dispersion contours for both pairs of materials (Co/Py and uniform YIG/patterned YIG), which are calculated by the plane-wave method. In addition, refraction in the Co/Py system was studied with micromagnetic simulations.

Index Terms—Magnetodynamics, spin waves, collimation, antidots lattices.

I. INTRODUCTION

The propagation of spin waves (SWs) in ferromagnetic films, with the saturated magnetic field applied in the plane of the film, is highly anisotropic. The dispersion relation (frequency versus wave vector) for SWs varies with changes in direction of the wave vector with respect to the external magnetic field [Stancil 2009]. Such intrinsic anisotropy is typical for magnonic systems [Gieniusz 2013]. The anisotropy of propagation can also be introduced by the periodic patterning of the ferromagnetic film [Tacchi 2015]. This leads to the breaking of the symmetry of the dispersion relation even for the configuration which has initially isotropic dispersion, i.e., for a homogeneous film with out-of-plane oriented magnetic field that is known as forward configuration.

The refraction effects on the interfaces between anisotropic media are complex and sometimes counterintuitive at specific conditions [Gralak 2000, Foteinopoulou 2003]. Such effects were intensively explored in photonic systems, where the most common way to introduce the anisotropy is the patterning of the structure in the form of a photonic crystal [Joannopoulos 2008]. Here, we adopt the ideas from photonics that are related to beam refraction [Luo 2002, Chigrin 2004] and collimation [Wu 2012] to magnonic systems, where the intrinsic anisotropy of solid film (absent in photonic systems) can also be exploited. The goal of this paper is to study the possibility of collimation for SWs propagating in thin ferromagnetic films, which is so far not completely utilized. In magnonics, the control of the SW's propagation direction has been discussed in connection with the caustic effect [Veerakumar 2006, Schneider 2010], where the *two* preferred directions of propagation exist. This is related to hyperbolic dispersion of in-plane magnetized thin films. We are interested in collimation, at which *only one* direction of propagation is supported. To achieve this effect, we need a system characterized by a dispersion relation which has a flat isofrequency dispersion contour (IFC) perpendicular to the required direction of the wave propagation. This can be obtained in a periodic system with a rectangular lattice with strong and weak coupling in two orthogonal directions [Kumar 2015]. In our study, we obtain suitable dispersion by applying a magnetic field in the plane of the system. It makes the propagation of SWs in orthogonal directions distinguishable (due to the introduction of anisotropic dipolar interactions). In addition, we show that a rectangular lattice is not necessary, and collimation can be obtained for the geometries of higher symmetry.

We consider two cases when collimation can appear: 1) due to the peculiar dispersion relation of homogeneous ferromagnetic film, and 2) due to the tailored magnetic properties of ferromagnetic film by its regular patterning. In the patterned medium, the dispersion relation of SWs can be shaped by adjusting the structural parameters. We show that the periodicity of the patterned medium enables all-angle collimation, i.e., beams incident on the interface between the homogeneous and the periodic medium may formally propagate along the normal direction in the exit medium even if the incidence angle is close to the 90° limit. We perform the analysis of the refraction with the aid of IFCs [Gralak 2006, Jiang 2012]. For the flat interface, the tangential component of the wave vector and, hence, the tangential component of the phase velocity must be conserved. The direction of the group velocity of the refracted wave can be found using this condition. It is determined by the direction normal to the IFC at the point on this contour, where the tangential component of the phase velocity is the same as in the medium from which the wave is incoming. In turn, the directions of incidence and refracted beams are given by the directions of the corresponding group velocities. Therefore, the direction of the beam refraction can be deduced by the geometrical analysis of the IFCs shape for two homogeneous media at the opposite sides of the flat interface. Similar analysis can be performed for the wave incident on the interface between homogeneous and periodic media. However, in this case, the wave vector can be shifted by any reciprocal lattice vector's tangential to the interface due to discrete translational symmetry along the interface. We have used this approach to adjust the geometry of the system, and to find the IFCs suitable for obtaining the all-angle collimation in yttrium–iron garnet (YIG)-based antidots lattice.

Corresponding author: J. W. Kłos (klos@amu.edu.pl).
Digital Object Identifier 10.1109/LMAG.2015.2494558

1949-307X © 2015 IEEE. Personal use is permitted, but republication/redistribution requires IEEE permission.
See http://www.ieee.org/publications_standards/publications/rights/index.html for more information.

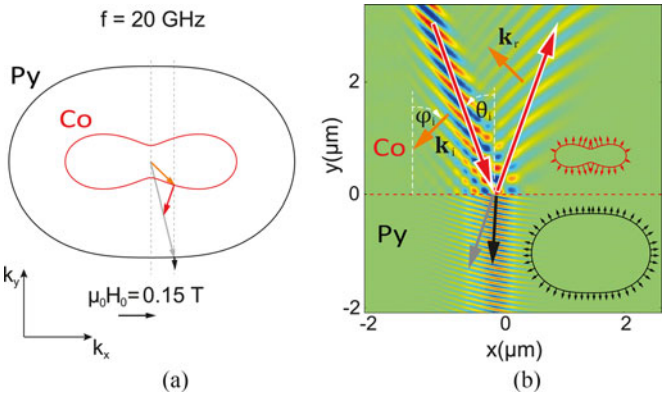

Fig. 1. Refraction of the SWs with frequency 20 GHz on the interface between Co and Py films (a) from dispersion results obtained by using PWM and (b) from MSs where the amplitude of the out-of-plane component of magnetization was visualized. The thickness of the films is 12 nm; the external magnetic field (0.15 T) is applied along the interface. Directions of the incident and reflected beams are marked by red arrows, direction of the refracted beam is marked by black arrow, for Co and Py, respectively. The directions of phase velocity are marked by orange and gray arrows for Co and Py, respectively. θ_i and φ_i denote the angle of incidence and the angle spanned between wave-vector $\mathbf{k}_i$ and normal to the interface. Note the difference in the divergence of the outgoing beams in Co and Py.

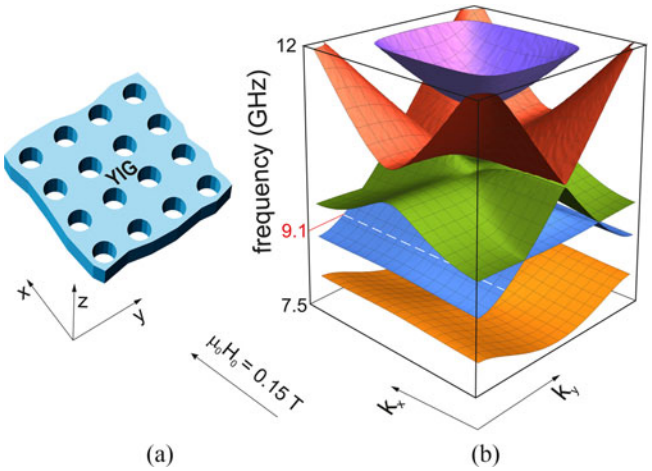

Fig. 2. (a) The structure of the magnonic antidots lattice in the form of YIG film of thickness 12 nm, patterned by cylindrical antidots (diameter 84.6 nm) arranged in a square lattice (lattice constant 150 nm). The values of magnetic parameters for YIG are: $M_S = 0.194 \times 10^6$ A/m, $A_{\text{ex}} = 0.40 \times 10^{-11}$ J/m. (b) Dispersion relation for the considered structure with external field applied along one principal direction of antidots lattice (i.e., x-direction), calculated using PWM. The figure presents the four lowest (and part of the fifth) magnonic bands over the whole first Brillouin zone. The white dashed line in (b) marks the IFC of the SW at 9.1 GHz.

In this paper, we will discuss the geometry of planar magnonic systems with a single internal interface. Then, we consider the SW dispersion and micromagnetic simulations (MSs) results for a system comprising only homogeneous films. Finally, we present a detailed analysis of dispersion for a system containing a square-lattice magnonic crystal.

II. MODEL

We consider two planar systems that consist of two half-planes. The first system is composed of two uniform half-planes of Co and Permalloy (Py) films [see Fig. 1(b)]. For this system, the collimation is limited to some range of incidence angles of SWs propagating from the side of Co. In turn, the all-angle collimation is shown for the structure made of the YIG with one half-plane in the form of a homogeneous film and the second half-plane in the form of a square lattice of cylindrical antidots [see Figs. 2(a) and 3(c)]. The interface with solid YIG is along one of the principal directions of the square lattice, i.e. is parallel to the *x*-axis. The magnetic field H_0 is applied along the interface for both systems.

To describe the SW dynamics, we used the Landau–Lifshitz equation (LLE) including the exchange and dipolar interactions. The 2-D dispersion relations (for both homogeneous and patterned media) were calculated using the plane-wave method (PWM) for the saturation state of the static magnetization [Rychły 2015]. The simulations of refraction and reflection of the Gaussian beams were performed with the aid of MSs using MuMax3 [Vansteenkiste 2014] package, solving the full LLE based on the finite-difference time-domain method. The detailed algorithm of MSs and especially description of Gaussian beams of SWs generation in MSs is presented in [Gruszecki 2015].

III. RESULTS AND DISCUSSION

The collimation effect can be observed for a magnetic planar system without periodic patterning. Fig. 1 presents the simulated refraction of the Gaussian beam of SWs on the interface between Co and Py. Both materials, and especially Co, are anisotropic in terms of SW propagation. The other factor that increases the anisotropy of Co (in reference to Py) is the fact that the selected frequency, 20 GHz, is much closer to the ferromagnetic resonance (FMR) frequency of Co than that of Py, due to higher magnetization saturation. As a result, we observe the highly anisotropic IFC for Co [drawn in red in Fig. 1(a)], exhibiting hyperbolic sections. The IFC for Py has a stadium-like shape. To observe the collimation of SWs incident from Co after refraction at the interface with Py, we use the nearly flat sections of the stadium-like IFC [drawn in blue in Fig. 1(a)]. However, the observed collimation is restricted here to some range of incidence angles around the direction normal to the interface, i.e., for the SWs with small tangential component of the phase velocity. This condition means that we are using the hyperbolic section of the IFC in Co in order to obtain the collimation in Py. The limited collimation incidence angle is close to the parabolic point [Chigrin 2004] of IFCs, which delimits the areas of the hyperbolic dispersion.

Fig. 1(b) demonstrates refraction and reflection of the SW's Gaussian beam at the interface between the Co and Py thin films which are simulated with the aid of the Mumax3 package. Both films were 12 nm thick, 8 μm wide, and 8 μm long (discretized using 8 nm $\times$ 8 nm $\times$ 12 nm rectangular unit cells), adjusting each other at one straight horizontal interface. The system was assumed to be uniformly and stably magnetized, and simulated under the presence of a small (0.15 T) static in-plane magnetic field directed parallel to the interface. In the Co film, far from the edges, the Gaussian beam of the SWs was

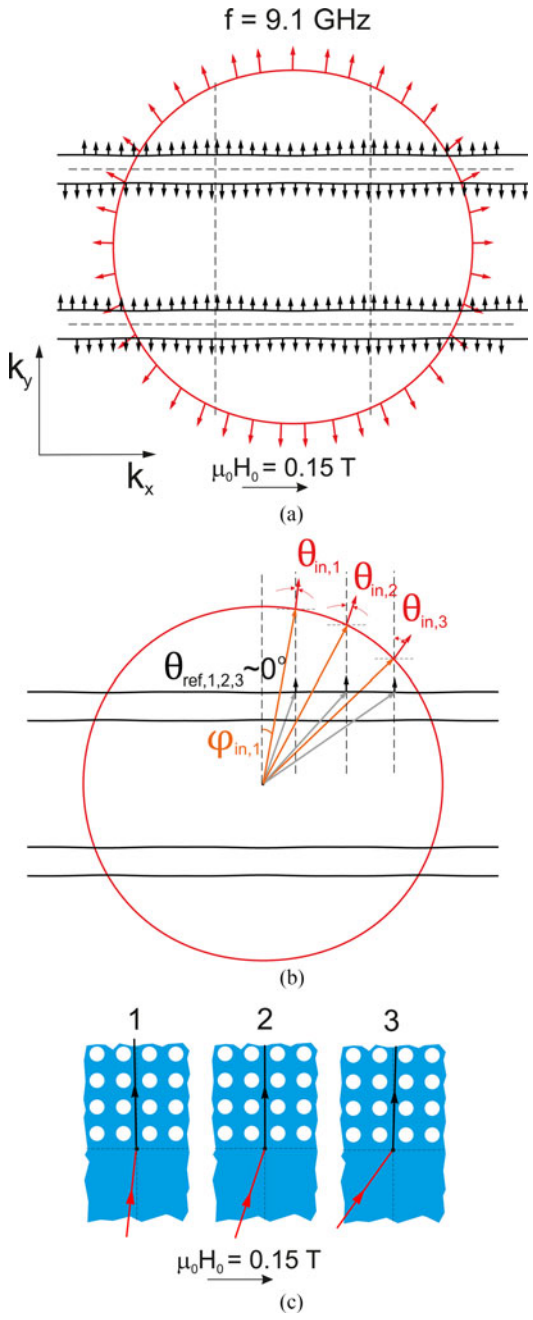

Fig. 3. (a) The IFCs for the antidots lattice presented in Fig. 2(a) and solid thin film of YIG at the frequency 9.1 GHz are shown in the wave vector plane with black and red solid lines, respectively. Arrows show the directions of the group velocity at different values of k_x. (b), (c) Schematics of all-angle collimation effect arising due to the flat IFCs for antidots lattice; beams coming from the solid film side are collimated in the patterned YIG film with antidots lattice into one beam propagating along the normal to the virtual interface ($\theta_{\text{ref}} = 0$), independent of the incidence angle θ_{in}. The angle φ_{in} corresponds to the angle spanned between exemplary wave vector (or phase velocity) of incident SWs and normal to the interface.

continuously excited with the width of $0.5\ \mu$m and at the frequency $f = 20$ GHz. The wave vector of the incident beam $\mathbf{k}_{\text{i}}$ creates an angle $\varphi_i = 45^\circ$ with the normal to the interface. To stay in the linear regime, the amplitude of the excitation was much smaller than the saturation magnetization of Co. In calculations, typical magnetic parameters were assumed: saturation magnetizations $M_{\text{S,Co}} = 1.45 \times 10^6$ A/m, $M_{\text{S,Py}} = 0.7 \times 10^6$ A/m, and exchange constants $A_{\text{ex,Co}} = 3 \times 10^{-11}$ J/m, $A_{\text{ex,Py}} = 1.1 \times 10^{-11}$ J/m for Co and Py, respectively. Simulations of the SW's propagation were carried out at a finite value of the damping parameter $\alpha = 0.0005$ for the Co and Py films.

In Co, the phase velocity of SWs (marked by orange arrow, being perpendicular to the wave-fronts and parallel to the wave vector $\mathbf{k}_{\text{i}}$) is almost perpendicular to the group velocity (marked by red arrow and denoting the direction of an energy propagation); see Fig. 1(b). This effect is a result of the hyperbolic-like IFC [see red line in Fig. 1(a)] occurring in Co with the chosen parameters. Similar analysis of MSs' results and IFC of Py shows that the angle between group and phase velocities is much smaller, but still significant. As seen in Fig. 1(b), the group velocity in Py is almost perpendicular to the interface in a range of the angles φ_i up to $\sim 60^\circ$. This can be concluded from Fig. 1(a), and was confirmed by multiple MSs for various angles of incidence.

The difference in the divergence of the beams propagating in Co and Py is worth noticing. It results from different values of phase velocities for SWs of the same frequency in Co and Py. On both sides of the Co/Py interface, we then have different ratios of wavelength to width for spin wave beam, i.e., in the case of Co the ratio is greater and due to that divergence of beam is stronger [Saleh 2007]. Nevertheless, in metallic ferromagnets, especially in Co, the damping is high. This significantly limits the proposed collimation scenario for practical realization.

Collimation of SWs can be obtained, and the mentioned restriction related to damping can be mitigated with the use of magnonic crystals based on thin YIG film [Yu 2014]. The 2-D plot of the dispersion relation of the planar square antidots lattice based on YIG film in Fig. 2(a) is presented in Fig. 2(b). For the magnetic field applied in-plane, the dispersion is strongly anisotropic for lower magnonic bands [Kłos 2012], where dipolar interactions prevail over the exchange ones.

The magnetic field applied in the *x*-direction supports the propagation of SWs (nonzero slope of the dispersion relation) along the *y*-direction in the low-frequency range. This is mostly caused by the profile of demagnetizing field lowering the effective magnetic field in the rows between antidots [Tacchi 2015] which are aligned in the *y*-direction. It is also clearly visible in Fig. 2(b), where the narrower frequency gaps and wider bands resulting in larger group velocities are observed along this direction. The top of the first band and the bottom of the second band have a peculiar shape, i.e., the dispersion is almost independent of the k_{x} component of the wave vector. This means that the group velocity, being the gradient of the dispersion relation, is directed almost exactly along the *y*-direction, independent of the direction of the corresponding phase velocity. The Bloch waves of different **k**-vectors will then propagate mostly in the *y*-direction, enabling collimation.

To investigate this effect, we have considered the refraction of the plane waves entering the patterned YIG film from the homogeneous region of this material. We have chosen arbitrarily one of the frequencies (9.1 GHz) lying within the second band in the center of the region, where the frequency of SWs is almost independent of k_{x} and varies almost linearly with k_{y} [see white

dashed line in Fig. 2(b)]. The top of the first band could also be considered to gain this effect, but this band is much narrower and characterized by lower group velocities and much narrower range of linear dependence of the frequency on the k_y component of the wave vector. This basically limits its application to the collimation of monochromatic beams only.

Fig. 3(a) presents the IFCs for the homogeneous film of YIG (red line) and for the patterned one [see black lines, extracted from the magnonic band structure shown in Fig. 2(b)]. The IFC for the homogeneous layer of YIG is approximately circular because of the weak intrinsic anisotropy. It is caused by small magnetization saturation of YIG and a comparatively high value of the considered frequency, which is significantly above the FMR frequency. Therefore, the phase velocity and group velocity are almost *collinear* for the SWs at this and higher frequencies.

The IFCs at 9.1 GHz for the antidots lattice in Fig. 3(a) are approximately straight and stretch between the boundaries of the first Brillouin zone. Due to the periodicity of the dispersion relation independent of the wave vector, the IFCs are extended infinitely in the reciprocal space, without any gaps. Also, the group velocity (marked by black arrows) almost coincides with one of two opposite directions (*y* or –*y*) and has a nearly constant value at any point of the IFC. This peculiar shape of the IFC is responsible for all-angle collimation. In addition, there is no restriction regarding the tangential component of the phase velocity that would result from the dispersion of the patterned YIG, and make this effect impossible to obtain. Therefore, the SWs incoming from the homogeneous YIG propagate in the direction normal to the interface, independent of their incidence angle. It is illustrated in Fig. 3(b), where IFCs are shown together with directions of the phase and group velocities in the media on both sides of the virtual interface, for three selected incidence angles. One more illustration of the collimation effect is schematically presented in Fig. 3(c), where the directions of incident and refracted waves are imposed on the sketch of the considered structure. The studies based on geometrical analysis of the shape of IFCs can be supplemented by the MS's results for the refraction of Gaussian beams, as it was done above for the interface of two homogenous materials, i.e., Co and Py.

IV. CONCLUSION

We have demonstrated the effect of all-angle collimation for SWs in a YIG-based square-lattice magnonic crystal. It is shown that for the SWs incident from the homogeneous region of YIG at an arbitrary angle, the outgoing wave propagates in the properly patterned area of the same material in the normal direction. This enables collimation without any restriction, except for that related to the coupling efficiency at the virtual interface. We supplemented this investigation by the analysis of SW refraction on the interface between two homogeneous materials: Co and Py. It was found that in this structure, the collimation effect can exist in a limited range of the incidence angle variation, being caused by intrinsic anisotropy of the magnetic films.

ACKNOWLEDGMENT

This work was supported by Polish National Science Centre under Project DEC-2-12/07/E/ST3/00538 and the EU's Horizon2020 program under the Marie Skłodowska-Curie Grant 644348.

REFERENCES

Chigrin D N (2004), "Radiation pattern of a classical dipole in a photonic crystal: Photon focusing," *Phys. Rev. E*, vol. 70, 056611, doi: 10.1103/PhysRevE.70.056611.

Foteinopoulou S, Soukoulis C M (2005), "Electromagnetic wave propagation in two-dimensional photonic crystals: A study of anomalous refractive effects," *Phys. Rev. B*, vol. 72, 165112, doi: 10.1103/PhysRevB.72.165112.

Gieniusz R, Ulrichs H, Bessonov V D, Guzowska U, Stognii A I, Maziewski A (2013), "Single antidot as a passive way to create caustic spin-wave beams in yttrium iron garnet films," *Appl. Phys. Lett.*, vol. 102, 102409, doi: 10.1063/1.4795293.

Gralak B, Enoch S, Tayeb G (2000), "Anomalous refractive properties of photonic crystals," *J. Opt. Soc. Amer. A*, vol. 17, pp. 1012–1020, doi: 10.1364/JOSAA.17.001012.

Gralak B, Enoch S, Tayeb G (2006), "Superprism effects and EGB antenna applications," in *Metamaterials: Physics and Engineering Explorations*, Engheta N, Ziolkowski W R, Eds. New York, NY, USA: Wiley, pp. 261–284, ch. 10.

Gruszecki P, Dadoenkova Yu S, Dadoenkova N N, Lyubchanskii I L, Romero-Vivas J, Guslienko K Y, Krawczyk M (2015), "Influence of magnetic surface anisotropy on spin wave reflection from the edge of ferromagnetic film," *Phys. Rev. B*, vol. 92, 054427, doi: 10.1103/PhysRevB.92.054427.

Jiang B, Zhang Y, Wang Y, Liu A, Zheng W (2012), "Equi-frequency contour of photonic crystals with the extended Dirichlet-to-Neumann wave vector eigenvalue equation method," *J. Phys. D: Appl. Phys.*, vol. 45, 065304, doi: 10.1088/0022-3727/45/6/065304.

Joannopoulos J D, Johnson S G, Winn J N, Meade R D (2008), *Photonic Crystals: Molding the Flow of Light*. Princeton, NJ, USA: Princeton Univ. Press.

Kumar D, Adeyeye A O (2015), "Broadband and total autocollimation of spin waves using planar magnonic crystals," *J. Appl. Phys.*, vol. 117, 143901, doi: 10.1063/1.4917053.

Kłos J W, Sokolovskyy M L, Mamica S, Krawczyk M (2012), "The impact of the lattice symmetry and the inclusion shape on the spectrum of 2D magnonic crystals," *J. Appl. Phys.*, vol. 111, 123910, doi: 10.1063/1.4729559.

Luo C, Johnson S G, Joannopoulos J D, Pendry J B (2002), "All-angle negative refraction without negative effective index," *Phys. Rev. B*, vol. 65, 201104, doi: 10.1103/PhysRevB.65.201104.

Rychły J, Gruszecki P, Mruczkiewicz M, Kłos J W, Mamica S, Krawczyk M (2015), "Magnonic crystals—Prospective structures for shaping spin waves in nanoscale," *Low Temp. Phys.*, vol. 41, pp. 745–759, doi: 10.1063/1.4932348.

Saleh B E A, Teich M C (2007), "Beam optics" in *Fundamentals of Photonics*, 2nd ed. New York, NY, USA: Wiley, pp. 75–85, ch. 3.

Schneider T, Serga A A, Chumak A V, Sandweg C W, Trudel S, Wolff S, Kostylev M P, Tiberkevich V S, Slavin A N, Hillebrands B (2010), "Nondiffractive subwavelength wave beams in a medium with externally controlled anisotropy," *Phys. Rev. Lett.*, vol. 104, 197203, doi: 10.1103/PhysRevLett.104.197203.

Stancil D D, Prabhakar A (2009), *Spin Waves—Theory and Applications*. New York, NY, USA: Springer.

Tacchi S, Gruszecki P, Madami M, Carlotti G, Kłos J W, Krawczyk M, Adeyeye A, Gubbiotti G (2015), "Universal dependence of the spin wave band structure on the geometrical characteristics of two-dimensional magnonic crystals," *Sci. Rep.*, vol. 5, 10367, doi: 10.1038/srep10367.

Vansteenkiste A, Leliaert J, Dvornik M, Helsen M, Garcia-Sanchez F, Van Waeyenberge B (2014), "The design and verification of MuMax3," *AIP Adv.*, vol. 4, 107133, doi: 10.1063/1.4899186.

Veerakumar V, Camley R E (2006), "Focusing of spin waves in YIG thin films," *IEEE Trans. Magn.*, vol. 42, pp. 3318–3320, doi: 10.1109/TMAG.2006.879624.

Wu Z H, Xie K, Yang H J, Jiang P, He X J (2012), "All-angle self-collimation in two-dimensional rhombic-lattice photonic crystals," *J. Opt. A*, vol. 14, 015002, doi: 10.1088/2040-8978/14/1/015002.

Yu H, d'Allivy Kelly O, Cros V, Bernard R, Bortolotti P, Anane A, Brandl F, Huber R, Stasinopoulos I, Grundler D (2014) "Magnetic thin-film insulator with ultra-low spin wave damping for coherent nanomagnonics," *Sci. Rep.*, vol. 4, 6848, doi: 10.1038/srep06848.